

Spatial characterization of planar deformation features in quartz and implications for understanding shock wave propagation at the grain scale

Anna Losiak¹, Izabela Gołębiowska², Ludovic Ferrière³, Jacek Wojciechowski⁴, Matthew Huber¹ and Christian Koeberl^{1,3}

¹Department of Lithospheric Research, University of Vienna, Althanstrasse 14, A-1090 Vienna, Austria (anna.losiak@univie.ac.at),

²Wydział Geografii i Studiów Regionalnych, University of Warsaw, Poland.

³Natural History Museum, Burgring 7, A-1010 Vienna, Austria.

⁴Smart Information Systems GmbH, Austria.

ABSTRACT

Planar deformation features (PDFs) in quartz are one of the most important diagnostic features that allow for the unambiguous identification of a meteorite impact structure. Previous studies of PDFs were either based on single grains or on a randomly chosen quartz grain "population". With this approach it was not possible to detect possible spatial relationships between quartz grains and PDFs developed within them. Here we investigate the spatial relations between a statistically significant number of grains (278) with PDFs (409) within a given area of a single thin section ($\sim 35 \text{ mm}^2$) from the Bosumtwi impact crater.

Some of the PDFs patterns and clusters (consisting of quartz grains with the same PDF orientation present) that we observed are suggestive of a heterogeneous shock field, very similar to one recently modeled numerically. Additionally, PDFs developed along different planes within the crystal lattice differ in their physical characteristics, appearance, and location within a grain. The PDFs developed along the $\{10\bar{1}3\}$ orientation are very well visible, thick and commonly cover a significant area of the grain. The PDFs developed along the $\{10\bar{1}1\}$ and $\{11\bar{2}2\}$ orientations are very short, faint and hardly visible under the universal-stage microscope. This difference was not noted in previous studies; it is likely that this indicates that different PDF orientations are formed in a somewhat different way.

We also present a new web-based program for indexing of PDF sets.

1. Introduction

There are only few diagnostic features that allow for the unambiguous identification of a meteorite impact structure (for a detailed review, see, e.g., French and

Koeberl 2010); including the preservation of meteorite fragments within a crater structure, a specific chemical and/or isotopic signature, the occurrence of shatter cones, shocked minerals, high-pressure minerals/phases, and/or diaplectic glasses. The most commonly used diagnostic feature for the confirmation of an impact structure on Earth is the occurrence of planar deformation features (PDFs) in quartz grains. PDFs are straight, parallel sets of planes of (amorphous) material that form along specific crystallographic planes in minerals and that are less than 2 μm wide and spaced 2-10 μm apart (e.g., Stöffler and Langenhorst 1994, Grieve et al. 1996 and references therein). Additionally, specific (combinations of) PDF orientations provide information on the peak shock pressure that is recorded by the rock, within the range of ~5 to 35 GPa, depending of the lithology (e.g., Hörz 1968, Grieve and Robertson 1976, Gratz et al. 1992, Stöffler and Langenhorst 1994, Huffman and Reimold 1996, Dressler et al. 1998, Ferrière et al. 2008, Holm et al. 2011).

Even though PDFs in quartz typically form along specific crystallographic orientations, their formation mechanism is still not well understood. Many hypotheses have been proposed, including 1) PDFs being traces of glide planes that developed within the quartz crystals to release stress (Engelhardt and Bertsch 1969); 2) PDFs being formed by heterogeneous response of the crystal lattice to the shock compression of high strength (Grady 1980), 3) PDFs are the result of the crystal lattice collapse along specific planes with lower (than average) shear resistance in the shock conditions and crystal lattice compensation caused by misfit on both sides of the shock front (Goltrant et al. 1992), 4) a combination of previously proposed models (e.g., Langenhorst 1994, Trepmann 2008).

The determination of the orientation of PDFs is usually done using a universal-stage (U-stage) mounted on a petrographic microscope, followed by the indexation of the measurements to crystallographic orientations in relation to the c-axis of the grains (e.g., Ferrière et al. 2009), or with the use of transmission electron microscopy (TEM; e.g., Goltrant et al. 1991). Currently, U-stage data are usually indexed manually, using a Wulff stereonet and following a strict procedure (e.g., Ferrière et al. 2009 and references therein). This procedure is both time consuming and error-prone, which somewhat also limits the usability and frequency of usage of this method. Additionally, because of the limitations of this method, only information about polar angles and Miller-Bravais indices of PDFs were recorded and used in previous studies (with a few exceptions, e.g., Walzebuck and Engelhardt 1979, Langenhorst and Deutsch 1994, Trepmann and Spray 2005). The angular relationships between PDF sets in a single given quartz grain were in most cases ignored. Recently, a new Excel©-based program for indexing PDFs has been developed by Huber et al. (2011). However, even though this program is much more accurate and faster than the manual (graphical) method, also allowing for the control of the error used in the calculation and the removal of human error from the plotting process, it does not provide information on the full angular relationships between PDF sets and it also cannot easily be used by, e.g., Macintosh users.

Previous studies on the development of PDFs or on the estimation of recorded peak shock pressures were either focused on single grains or on a randomly chosen quartz grain "population" (e.g., Langenhorst and Deutsch 1994, Ferrière et al. 2008). Up

to now, no study investigated the spatial relations between a statistically significant number of grains with PDFs within a given thin section area. The aim of the present work is 1) to investigate the spatial relations between PDFs developed in all quartz grains that are visible within an area of $\sim 35 \text{ mm}^2$ of a thin section, 2) to introduce a web-based program for PDF indexing that allows the analysis of azimuthal angles between different PDFs in a given quartz grain, and 3) to better understand the shock wave propagation mechanisms at the thin-section scale and the formation mechanism of PDFs.

2. Methods

2.1 Sample investigated

To evaluate the spatial relationships between PDFs at the thin section scale, one thin section of a highly shocked rock from the Bosumtwi impact crater was used. Bosumtwi is a 10.5 km in diameter, well preserved, 1.07 Ma old impact crater located in Ghana (see, e.g., Koeberl et al. 2007). Sample KR8-029 was previously studied by Ferrière et al. (2008) and comes from a depth of 271.4 m (LB-08A drill core), from the shocked basement rocks of the crater. This sample is a coarse-grained meta-greywacke with the largest grains, quartz and feldspars, being up to few millimeters in size. It consists of (modal analysis from Ferrière et al. 2008): 46.4 vol.% quartz 23.7 vol.% alkali feldspar, 10.8 vol.% plagioclase, 4.7 vol.% chlorite, 3.6 vol.% calcite, 1.7 vol.% opaques, 1.3 vol.% muscovite, 0.6 vol.% "other minerals" (including e.g., epidote, amphibole, sphene, etc.), and 6.5 vol.% of matrix (i.e., all grains smaller than $50 \mu\text{m}$). According to Ferrière et al. (2008), based on counting using a petrographic microscope, 58% of the quartz grains in this thin section show evidence of shock, and 90.8% of these shocked grains display PDFs (the other 9.2% displaying planar fractures, PFs).

This sample was selected for our study because of: 1) the abundance of relatively large quartz grains, 2) most quartz grains occur in aggregates, and 3) the high proportion of shocked quartz grains (mainly with PDFs).

2.2 Methods used

At first, all visible PDFs in all the quartz grains within a restricted area were investigated using the U-stage. In total, the properties of 278 grains (directions of their c-axis and of the PDFs) were measured along with their position on the thin section. All grains were measured with respect to the same coordinate system, defined by the microscope axis and the orientation of the thin section with respect to the U-stage (Fig. 1). Repeated measurements of the same grains showed that the error between measurements of planar features is at maximum of 4° . In a second step, PDFs were indexed with the computer program presented here (see below). The generated data for all the grains were then inserted into a database that was linked to a thin section map (prepared with an optical microscopy microphotograph) using a geographic information systems software (GIS). Spatial analysis of the grains and PDFs characteristics was performed using the ArcGIS 10 software produced by ESRI (Kennedy 2001).

Additionally, part of the statistical analysis was carried out using the Statistical Package for the Social Sciences (SPSS) 14.0 for Windows developed by IBM.

The limitations of the applied methods are as follows: 1) detailed observations using scanning electron microscope (SEM) of some of the grains previously investigated under the optical microscope have revealed that additional PDF sets, not visible and thus not measured with the U-stage, occur. This implies that some of the grains that were described as "unshocked" (i.e., free of PDFs) contain PDFs; 2) the U-stage do not allow the determination of the full information on the crystal lattice properties (it is for example not possible to detect Dauphiné twins); 3) the sample size, even though a total of 278 grains were investigated in our study, is relatively limited, mainly due to the very time-consuming nature of performing the U-stage measurements; 4) the study is based on one thin section that was prepared from a three-dimensional rock, which may introduce further limitations.

2.3 Development of a web-based program for indexing PDFs

2.3.1 Description of our program for indexing PDFs

To evaluate the data generated here, and to provide a tool for the community, we developed a web-based program for indexing PDFs. The program is designed to evaluate data from U-stage measurements to quickly assess the relationships between the c-axis and the various PDFs within a given grain. This evaluation is then compared to angles of known, typical, PDFs in quartz (as defined in Ferrière et al. 2009, and references therein). The presented approach simplifies the mathematical calculations required for indexing and allows removing errors related to some distortions that may be induced when representing information derived from a three-dimensional (3D) crystal on a 2D Wulff stereonet.

To properly index PDF sets, two pieces of information are mandatory: 1) the polar angle between the c-axis and the measured feature, and 2) the azimuthal angle between the a-axis and a PDF set. As the a-axis cannot be determined with the U-stage (although this is possible with an Electron Back-Scatter Diffraction-system), an approximation is typically used, namely the angular relationship between two (or more) sets of non-basal PDFs are compared, which can then be used to determine the orientation of the a-axis.

For each quartz grain, U-stage measurements provide angular coordinates (azimuth and inclination) of the c-axis and of all visible PDFs. The program is based on a set of equations that allow the transformation of the coordinates for each grain, from microscope-oriented coordinates to crystal structure-oriented coordinates (Fig. 1). The program essentially "rotates" a grain to have the c-axis coincide with the central axis of the sphere used for the indexing (i.e., the c-axis' inclination angle becomes 90°) and corresponding transformations are applied to all planar features determined in the given grain (Fig. 1), mathematically mimicking the manual process that would be performed with the Wulff stereonet.

The following equations were used to transform the coordinates systems, related to the cosine and sine rules of a spherical triangle:

$$(1) \sin(\delta) = \sin(a)\sin(\varphi) + \cos(a)\cos(\varphi)\cos(A)$$

$$(2) \sin(H) = -\sin(A)\cos(a)/\cos(\delta)$$

$$(3) \cos(H) = [\sin(a) - \sin(\delta)\sin(\varphi)]/\cos(\delta)\cos(\varphi)$$

Where δ is 90° minus the polar angle of the measured planar feature; a is the measured inclination of the planar feature, φ is the measured inclination of the c-axis, A is the azimuthal distance between the c-axis and the planar feature, and H is the azimuthal angle of the planar feature. After performing the transformation described above on the measured PDFs, the relative angular relationships of the PDFs within a grain can be read directly from their coordinates.

The algorithm is designed to find if relative angular relationships between measured features are consistent with the model angular relationships of PDFs as described by Ferrière et al. (2009). This operation consists of four steps (Fig. 2). First, the measured planar features are indexed using only the polar angle data by comparing calculated values of polar angles with values of polar angles of known PDFs. If no typical orientation corresponds to a known PDF for a calculated polar angle, the measured planar feature is rejected and not used for further computation, and marked as "unindexed". For all of the remaining features, one or more known PDF classifications are assigned (this is called here the initial classification). If a single planar feature was measured within a given grain, or also in the case that only one other planar feature was indexed as a set of basal PDF (0001) based on its polar angle, the program will already achieve the calculation for this grain at this step. The final display will then indicate that this set of PDF was indexed only based on its polar angle.

During the second step, the program compares the angle between measured sets of PDFs in the grain to known typical PDFs. The expected classification of measured PDFs based on the polar angle (step 1) is used to generate the possible and expected azimuthal angles between two sets of PDFs. For example, if two measured features were classified as $\{10\bar{1}3\}$ and $\{10\bar{1}2\}$ orientations in the first step, the only possible azimuthal differences between them are: 60° , 120° , 180° , 240° , and 300° (\pm error size). If the program finds that the measurements do not fall within these expectations, then, only one set of PDF (i.e., the one with the smaller polar angle error) is indexed, while the other set of PDF is considered to be unindexed. In many cases, more than one combination of indexed PDFs is possible; e.g., some PDFs can be indexed either as $\{10\bar{1}3\}$ & $\{10\bar{1}3\}$ orientations or as $\{10\bar{1}3\}$ & $\{10\bar{1}4\}$ orientations. In this specific case, the program takes into account all possible combinations of PDF sets.

The third step of the algorithm consists in the calculation of the errors for each of the possible classifications by summing up all angular differences between known PDF orientations and measured orientations of PDFs.

Finally, the combination of PDF sets with the lowest error is chosen as the proper indexed orientation; however, all other possible combinations are also listed in the detailed results table.

2.3.2 Input & Output

For the data input, the user has the choice between a .csv file (coma-delimited) or a .txt file. An example of an input file, with detailed instructions, is available online together with our program. Each line of the input file corresponds to a set of numbers describing a single quartz grain. The measured angular data can be entered as a range of values (minimum and maximum measured values; “min-max”). If the c-axis was determined to be vertical during measurements it should be converted manually to the horizontal position (e.g., by "subtracting" 90° from the inclination and by correcting the azimuth by 180°; or the easiest is to change W to E (or E to W) and to "subtract" 90° from the inclination; the corresponding PDFs measurements should, in any case, be altered). There are no limitations on the total number of grains in the dataset, or on the number of features/PDFs per grain. If there is an error in the input data (e.g., an inappropriate number of PDFs in relation to the number of input columns), an error message describing the type of problem will be displayed.

Results can be exported as csv and/or jpg files. The results are presented as follows: 1) a main result table with the best possible combination of PDFs orientations for each grain, 2) a detailed results table with input and output data together with all possible combinations of PDFs orientations, 3) aggregated result tables, 4) aggregated plots, and 5) diagrams for all measured PDFs and also for each grains. The presentation of the results is similar to what is commonly presented in the literature (e.g., Grieve et al. 1996, Ferrière et al. 2009). Additionally, a detailed log of the performed computations is available for each single grains, including detailed information on polar angle, compared azimuthal angles, and all possible combinations of PDF indices.

In addition, two different types of options are available for the calculation, the so-called "error handling" and "error level". "Error handling" specifies how the program interprets data input with a range of values for the c-axis and the sets of PDFs in a given grain. There are two modes of "error handling" for the dataset: 1) "Average": the algorithm calculates the average value of the entire measured interval, and the indexing is performed using this "average value"; 2) "Min-max": values from the entire interval are considered in the subsequent computations. Using this second setting, a PDF will be indexed if any part of the measured interval matches a known, typical, PDF orientation. "Error level" describes the distance from a classified PDF orientation that will still be counted as properly indexed. It is recommended to use a 5° error level, as it is thought to be a level of error inherent to the optical microscopic measurements and have been typically used when plotted manually with the stereographic projection templates (e.g., Engelhardt and Bertsch 1969, Stöffler and Langenhorst 1994, Ferrière et al. 2009).

The comparison between the produced results using the different "error handling" options is shown in Fig. 3 and in Tab. 1. Table 1 shows that, no matter which method is used, the relative abundance of the different indexed PDF orientations does not change significantly. Additionally, the larger the error level, the more similar are results of the computing using different error handling options. Increasing the "error level" results in a significant decrease of the number of unindexed PDFs. For example, when applying an "average setting" and changing the "error level" from 3°, 5°, to 7°, the number of unindexed PDFs decreases from 43 % through 19 % to only 9 % (see Tab. 1). Furthermore, the proportion of unindexed features/PDFs strongly depends on the error

handling method that is used for the calculation; for example, the proportion of unindexed features will increase from 5 % to 19 % just by changing the error handling method used, from the “Min-max” to the “Average” method. Results obtained using the “Min-max” method with a 5° error level and the “Average” method with a 7° error level are usually very similar. This suggests that the average uncertainty on the measurements in this study using the U-stage is at least of 4°.

2.3.3 Comparison between the “manual” and “automatic” methods for PDF indexing

To test and validate our program we compared the results generated by our program (using the “Min-max” method and 5° error level) with those obtained with the manual (graphical) method. For this purpose, we have used data obtained from five samples from different impact structures (see Tab. 2).

The results obtained using the program (“automatic”) and the manual method are almost identical. The differences in absolute frequency percentage are negligible and too insignificant to influence inferences on the shock pressure during impact cratering (e.g., Stöffler and Langenhorst 1994). These minor discrepancies between the manual and automatic methods can have several origins. First, a human operator is more prone to index a feature that is near the boundary (i.e., almost indexed), while the program is very strict. Second, the human operator and the program can choose different Miller-Bravais indices for certain grains, for example, when two PDF sets can be indexed either as $\{10\bar{1}1\}$ & $\{22\bar{4}1\}$ orientations or as $\{11\bar{2}2\}$ & $\{40\bar{4}1\}$ orientations. Due to the lack of a-axis data, it is in fact impossible to differentiate between these two combinations, and the program will choose the option with the smallest cumulative error. Third, it seems that the projection that is used for the manual indexing tends to over-index PDFs with low polar angles. In addition, the manual method does not take into account the full measured interval for the c-axis orientation (Ferrière et al. 2009), while our program does. Finally, even the most accurate and precise human operator will make mistakes due to the wearisome nature of the manual indexing method. The comparison of the PDFs indexed by hand and using the program (Tab. 2) shows that the automatic method of indexing gives very comparable results to the ones obtained by an experienced researcher (L. F.); however, based on the nature of the automated algorithm, the results are more precise and reproducible.

The program that was developed for this study is available online at: www.MeteorImpactOnEarth.com/ustage/program.html. The source code (i.e., implementation in Java programming language) is also available upon request from the authors.

3. Results

In total, 278 quartz grains from an area of 34 mm² were measured with an U-stage. 219 of these quartz grains display 1 to 5 indexed PDF sets (Fig. 4-7). The mean number of PDF sets per grain is 2.03 (relative to the shocked quartz grains only) and is 1.47 (if all investigated quartz grains are counted; i.e., including also unshocked grains).

Based on GIS analysis, the measured quartz grains are relatively homogenous in size, with an average area of the grains of $\sim 33 \mu\text{m}^2$. However, the difference between the largest ($295 \mu\text{m}^2$) and the smallest ($2 \mu\text{m}^2$) grains is significant. At the thin section scale, the quartz grains are distributed within twelve unequally sized "clusters" (Fig. 6, Tab. 4). Cluster #6 is the largest of all; it consists of 52 grains with 75 indexed PDFs. Clusters #4 and #7 are the smallest ones, with 9 and 12 grains and 14 and 12 PDFs, respectively (Fig. 6). Table 3 gives the details concerning the number, mean values, and standard deviations of the number of grains and PDFs in each cluster. Figure 7 shows the distribution of clusters and quartz grains (along with information on the number and orientation of PDFs) within the studied area of the thin section.

The orientation of 441 sets of planar features were measured and subsequently 408 PDFs were indexed using the "min-max" and 5° error level settings of the program described above (Tab. 3). Thirty three (representing 7.5 % of the total) of the measured features were unindexed, using the chosen settings. A detailed analysis of the grains with unindexed features revealed that, in most cases, these features would be in fact indexed if the error level were to be increased to 6° (instead of 5°). The most common PDF indices are: $\{10\bar{1}3\}$ (45.8 %) and $\{10\bar{1}4\}$ (23.4 %) (Fig. 5). Less frequent orientations of PDFs are $\{10\bar{1}1\}$ (8.2 %), $\{11\bar{2}2\}$ (4.1 %), and $\{10\bar{1}2\}$ (3.6 %). A total of only 3.4 % of the PDFs were indexed as basal (0001). A few other orientations of PDFs are also present, but represent less than 2 %.

4. Discussion

4.1 Sample characterization and comparison of results with previous data

The thin section used in the present study was previously analyzed by Ferrière et al. (2007, 2008) as part of a large study on the Bosumtwi impact crater for which 121 samples from the drill core LB-08A were analyzed. Comparing the results of the current study with previous work can help to better understand if, and how, our approach affects the results (Tab. 3). In the present study, using the U-stage and based on a restricted part of the thin section, a total of 78 % of the 278 investigated quartz grains were found to be shocked. This proportion is a much higher percentage than the 58 % (out of 508 grains counted) reported in Ferrière et al. (2008). However, Ferrière et al. (2008) obtained this value of shocked quartz grains using the optical microscope without U-stage; therefore, it is not really surprising that a higher proportion was detected in our study. Ferrière et al. (2008) also discussed the fact that PDF sets not observable under horizontal stage examination are visible when using the U-stage. They noted that the average number of PDF sets per grain is 28 ± 9 rel% higher when determined by U-stage. If we extrapolate this number, our present estimate of the number of shocked quartz grains is in good agreement with the work of Ferrière et al. (2008).

The largest difference between our study and the previous work by Ferrière et al. (2008) is in the percentage of PDFs indexed as $\{10\bar{1}3\}$ orientation; although they dominate (92 %) the sample set in Ferrière et al. (2008), they are much less common, only 46 %, in this study. One of the most likely cause of this apparent discrepancy is in part artificial and due to the different model PDFs matrix used for indexing. PDF

indexing by Ferrière et al. (2008) was done using the traditional template with 10 model PDF orientations as given, e.g., in Stöffler and Langenhorst (1994), while in this study, the scheme, with five additional characteristic crystallographic orientations, by Ferrière et al. (2009), was applied. As a result, the PDF orientation $\{10\bar{1}4\}$ was assigned to some features that would have been previously likely classified as $\{10\bar{1}3\}$ orientations (and in a few cases unindexed). Interestingly, Ferrière et al. (2008) did not find any PDF sets with the $\{10\bar{1}1\}$ orientation, while in our study this orientation represents 8 % of the measurements. The re-examination of the grains containing this orientation revealed that the PDFs with the $\{10\bar{1}1\}$ orientation tend to be less easily visible than other PDFs, and thus can in some cases be overlooked. The $\{10\bar{1}1\}$ along with $\{11\bar{2}2\}$ orientations are commonly poorly developed sets, hardly visible under the U-stage, and present on the grain margins as a few microns long planar and parallel features. This difference of physical characteristics, appearance, and location within grain of different PDFs orientations was not noted in previous research and indicates that different PDFs orientations may have developed under somewhat different conditions.

The average shock pressure is commonly determined based on PDF orientations in a given thin section/sample (see e.g., Hörz 1968, Grieve and Robertson 1976, Huffman and Reimold 1996). The average shock pressure estimates based on the PDF orientations measured in this study and by Ferrière et al. (2008) would be similar (Stöffler and Langenhorst 1994). However, because $\{10\bar{1}1\}$ orientation represents 8 % of PDFs measured in the current study, and is thought to develop at 5 GPa, the range of shock pressures estimated based on current measurements could be slightly lower than based on data from Ferrière et al. (2008).

4.2 Heterogeneous distribution of PDFs in quartz grains from the studied sample

There are three different ways in which the PDFs in quartz show a heterogeneous spatial distribution (see Fig. 8): First, as noted by Walzebuck and Engelhardt (1979) and Kieffer (1971), PDFs are distributed heterogeneously within single quartz grains (e.g., Fig. 9). One area within a particular grain can be bereft of any indication of shock metamorphism, while another area can be so thickly packed with multiple PDFs belonging to multiple orientations that it is somewhat difficult to clearly identify them, and their exact number. Those grains area are so damaged by shock that when seen under the cross-polarized light they look almost isotropic. The transition from the apparently "unshocked area" to the shocked area is very abrupt and happens over the scale of a few micrometers. This variability is probably related to pre-shock heterogeneity of the sample, particularly with regard to the collapse of the pore spaces due to shock wave propagation (Kieffer 1971, Kieffer et al. 1976, Güldemeister et al. 2013). Laboratory experiments also show that the local stress can range from half to twice in intensity when compared to the average shock pressure, even though it is clear that such experiments, done on single quartz crystals (Gratz et al. 1992), have some limitations compared to natural processes. Such a local intensity of stress may be the result of the intrinsic instabilities in the thermo-mechanical deformation process (Grady 1980).

Second, the spatial distribution of grains with a specific number of PDFs per grain-area is heterogeneous; in multiple cases, grains with very different numbers of PDFs

per grain-area are located close to each other (Fig. 7). For example, in our cluster #6, adjacent grains have either a very high or a very low number of PDFs per unit area in the grain. A similar heterogeneity within a single sample was observed by Dressler et al. (1998). This can be related to pre-impact heterogeneity (e.g., small pores or other impurities) in the cluster. The collapse of the pores during the passage of the shock wave could have caused reverberation and/or rarefaction of the shock wave(s), locally amplifying the average shock pressure (see e.g., Kieffer 1971, Bowden et al. 2000, Gldemeister et al. 2013). However, other clusters (e.g., #1, #2, or #12) are relatively consistent, with adjacent grains sharing similar number of PDFs per area. It appears that the stress field in these specific locations in the sample was relatively uniform. The relative homogeneity of these clusters might have been caused by pre-impact grains in these clusters strongly adhering to each other.

Third, heterogeneity is present at the cluster level. Quartz grains in the studied sample are grouped into 12 distinct clusters having between 9 and 52 grains (with an average between 20 and 30 grains). The average number of PDFs per all quartz grains (i.e., including the quartz grains that do not display PDFs) varies between 1.0 (in cluster #7) and 1.9 (in cluster #5) (see Tab. 4). These differences in the shock level recorded by the different clusters are probably caused by the lower level of heterogeneities described previously (i.e., at the sub-grain and grain level) and are likely a result of the semi-random distribution of high-pressure areas. This observation suggests that, depending on the location of the analyzed grains, the results (and thus the estimation of the average shock pressure) can vary by as much as a factor of two. This finding supports recommendations given by Ferrire et al. (2009) that in order to assure a proper estimation of the shock level in a given sample, it is important to measure a large number of PDF sets (optimally more than 100) from randomly chosen grains from different locations within a given thin section/sample.

In order to quantify the spatial relationships between the number of PDFs and the spatial relationships of the quartz grains at the scale of the thin section, various statistical tests were performed. The Pearson's product moment (r) statistical test (Rogerson 2001) measuring linear dependence between two variables (Devore and Peck 1997) was used to investigate the correlation between the number of PDFs per grain with two other variables: 1) the total area of a grain, and 2) the location with relation to the edge of a cluster. The Pearson's product moment varies from -1 to 0 to 1 (indicating, respectively: strong anti-correlation, no correlation, or strong correlation) and can be calculated using the following equation:

$$r = \frac{\sum z_x z_y}{n - 1}$$

where z_x and z_y are the z-scores (i.e., the distances from the mean expressed as units of standard deviation) associated with x and y variable, respectively, and n the number of observations.

The correlation coefficient calculated for the grain's area and the number of PDF orientations in each grain is 0.34 ($\alpha < 0.01$), indicating a strong positive correlation between the two variables. This correlation indicates that the larger the grain, the more PDF orientations it tends to include; this is in agreement with the findings of Walzebuck

and Engelhardt (1979), who noted that with increasing grain size, there is an increasing chance that heterogeneously distributed local stress maxima exceed the threshold pressure necessary for the formation of PDFs within a specific grain. In Figure 8, the average density (i.e., relative abundance in a given area) of PDF sets per grain-area is shown; there is an over-representation of the small quartz grains with a very high density of PDF sets per grain-area. These grains are commonly located in the inside part of the clusters, tightly surrounded by other quartz grains. In a few cases, their formation may be explained by the rotation of part of the crystal previously being part of a larger grain, due to extensive shock, as already suggested by Kieffer (1971). Other grains may show a strong correlation due to a calculation artifact (i.e., a single PDF set in one grain gives higher set density than 4 sets within a very large grain).

Kieffer (1971) and Dressler et al. (1997) suggested that quartz grains within a porous rock or embedded in a “soft” matrix are less likely to develop PDFs and/or PFs when compared to quartz grains in an uniformly “hard rock”. For this reason we tested the hypothesis that the most heavily shocked grains tend to be located in the inner part of the clusters. However, the result of the Pearson’s product moment correlation coefficient seems to indicate that there is no significant correlation between the number of PDFs and the percentage of matching grain borders with the boundary of a cluster (see Tab. 4). Only cluster #1 shows a medium negative correlation close to the 2 sigma level of significance. Therefore, there is no clear evidence that the development of PDFs is directly related to its surroundings (with the notable exception of the collapse of pore spaces). Grains are shocked in a similar way, regardless of whether they are surrounded by other “rigid” quartz grains or by fine-grained “soft” matrix.

In order to test the spatial variability of the shock effects (expressed by the grouping of grains with a similar number of PDFs) on a scale of a few hundreds of micrometers, the Anselin Local Moran’s test was applied (Anselin 1999, Rogerson 2001). This test allows detecting local spatial autocorrelation and can be used to identify local clustering (regions where adjacent areas have similar values) or spatial outliers (areas distinct from their neighbors). In this study the Anselin Local Moran’s test is used to identify clustering of grains with high number of PDFs (marked as HH on the Fig. 10), clustering of grains with small number of PDFs (marked as LL), and spatial outliers; e.g. grains with a high number of PDFs surrounded by grains with a small number of PDFs (marked as HL). In this analysis, only grains that share a boundary will influence computations of the central grain (*ArcGIS Help Library* 2010). The Local Moran’s statistic of spatial association is given by:

$$I_i = \frac{x_i \bar{X}}{S_i^2} \sum_{j=1, j \neq i}^n w_{i,j} (x_j - \bar{X})$$

where x_i is an attribute for the feature i , \bar{X} is the mean value for this attribute, $w_{i,j}$ is the spatial weight between features i and j , and with:

$$S_i^2 = \frac{\sum_{j=1, j \neq i}^n w_{i,j}}{n-1} - \bar{X}^2$$

where n is the total number of features.

The results of this analysis show that several grains yield statistically significant results (Fig. 10), thus, indicating that in some cases grains with high, or low, number of PDFs present are spatially clustered. However, it is necessary to take into account that due to the non-continuous space and very irregular shapes of the quartz grains, this analysis is complex and cannot be fully conclusive. Seven of our defined clusters can be categorized as HH, and only one cluster as LL. There are also four LH clusters. All of the LH grains are located on the edge of the clusters whereas the LL grains are located on the border of two clusters. However, because only very few of the measured quartz grains show a relation between the number of PDF sets present within them and within their neighbors, the number of PDF orientations in the grain does not seem to be dependent of the special location of the grain itself.

4.3 Non-random distribution of different PDF types/orientations

Our statistical analysis revealed that the number of PDF sets within a given quartz grain is likely related to a heterogeneous stress field developed during the impact event. However, the development of specific PDF orientations is potentially more systematic. The Getis-Ord General G statistical analysis is designed to measure the degree of clustering for either high values or low values of the tested variables (Getis 1999). This test was applied here to estimate the degree of clustering of each PDF orientations. In this analysis, all grains containing a specific indexed PDF orientation (e.g., $\{10\bar{1}1\}$) are assigned a value of “1”, grains without any PDFs or with PDFs with orientations other than the specific PDF orientation that is investigated are assigned a value of “0”. The General G statistic of overall spatial association is given as:

$$G = \frac{\sum_{i=1}^n \sum_{j=1}^n w_{i,j} x_i x_j}{\sum_{i=1}^n \sum_{j=1}^n x_i x_j}, \forall j \neq i$$

Where x_i and x_j are attribute values for features i and j , and $w_{i,j}$ is the spatial weight between feature i and j . The polygon contiguity conceptualization of spatial relationships is also selected while performing this statistic analysis. The Getis-Ord General G statistic test works best when there is a fairly even distribution of values and only few areas with high values of a variable (in our case a specific PDF set). In addition to the G value, p -value and z -score were also calculated. The p -value is the probability that the observed spatial pattern is created by a random process, and the z -score is the standard deviation. A very high or very low (negative) z -score associated with small p -values (below 0.10 confidence level) indicate that it is unlikely that the observed spatial pattern reflects a random pattern.

All PDF combinations were tested with the Getis-Ord General G statistic test; however, the results were significant only for $\{10\bar{1}1\}$ and $\{11\bar{2}2\}$ PDFs orientations (see Fig. 11). The clustering for the other orientations of PDFs cannot be determined because of statistical reasons; Some PDF orientations, such as $\{10\bar{1}3\}$ and $\{10\bar{1}4\}$ orientations are present in most of the grains, and, thus they appear as a large single cluster. However, this clustering is only an artifact of their abundance and is not in any

case meaningful, and thus cannot be analyzed further. On the other hand, other PDF orientations, such as the $\{3\bar{1}\bar{4}1\}$ orientation, are generally not abundant enough to allow a statistically meaningful analysis.

Grains with $\{10\bar{1}1\}$ orientations are characterized by the General G value of 0.023, z-score of 1.96, and p-value of 0.05 (Fig. 11). Results for the PDF orientation $\{11\bar{2}2\}$ indicates a slightly more clustered pattern, with observed General G value of 0.035, z-score of 2.11, and p-value of 0.04. Moreover, analysis of both of these PDF orientations together yields an even more clustered pattern with a general G value of 0.022, z-score of 2.38, and p-value of 0.0175 (close to the more conservative confidence level). The complete results are presented in Fig. 11. Based on this analysis, with 95% confidence level, we note that the clustered distribution of the $\{10\bar{1}1\}$ and $\{11\bar{2}2\}$ orientations is not random.

Based on this statistic test, we can argue that the development of specific PDF orientations is related to: 1) the orientation of the crystal lattice of the quartz grains with respect to the shock front (as already suggested by, e.g., Walzebeck and Engelhardt 1979, Langenhorst and Deutsch 1994), and 2) the peak shock pressure experienced by the sample (see e.g., Langenhorst and Deutsch 1994, Langenhorst 2002). The orientation of the crystal lattice does not seem to explain clustering of grains with specific PDF orientations observed in the studied sample. The $\{10\bar{1}1\}$ and $\{11\bar{2}2\}$ orientations are developed in neighboring grains, even though the crystallographic directions of the quartz grains in the studied sample are very different from each other (Fig. 7). For example, in cluster #1, grains that include $\{10\bar{1}1\}$ and/or $\{11\bar{2}2\}$ PDF sets have very different orientations of their crystal lattice. However, there are also grains that have a similar orientation of their crystal lattice (with less than 10 degrees of difference) to a grain displaying $\{10\bar{1}1\}$ and/or $\{11\bar{2}2\}$ PDF sets, but that do not show similar PDF orientations. The same observations can be made in other clusters. Therefore, we suggest that the orientation of the crystal lattice of the grains is likely not correlated with the development of a specific PDF orientation.

It is clear that in a heterogeneous, more or less porous, and multigranular sample from a large impact crater, the shock wave is much more complex than a shock wave produced experimentally in a single crystal sample in a laboratory experiment (e.g., Langenhorst and Deutsch 1994). Thus, heterogeneities of the sample (especially the collapse of pore spaces) can alter the direction and strength of the “initial” shock wave front, producing multiple overlapping/over-imposed shock waves that can travel in different directions (e.g., Kieffer 1971, Baratoux and Melosh 2003, Güldemeister et al. 2013). This implies that the existence of a unique direction of shock propagation influencing development of specific PDF orientations is not a realistic scenario in the case of a natural impact.

The strength of the shock pressure field experienced by a portion of a sample seems to explain the observed distribution of PDF orientations. Quartz grains that are located within an area experiencing the stress appropriate for the development of $\{10\bar{1}1\}$ and/or $\{11\bar{2}2\}$ orientations will contain them, despite the variable orientation of their crystal lattice. If the shock pressure was, either too high (i.e., above ~25 GPa), or too

low (i.e., lower than 5-10 GPa), these PDFs would not have formed (see, e.g., Langenhorst and Deutsch 1994).

4.4 Determination of the average shock pressure in quartz bearing impactites

Heterogeneities in the recorded shock effects already at the outcrop scale, but also at the sample or even at the thin section scale, draw attention to the question of representativeness of the estimated sample's "average shock pressure" based on PDFs measurements. The methodological problems in using the orientation of planar microstructures for the estimation of shock-pressures were previously pointed out by several authors, including Grieve et al. (1996) and Ferrière et al. (2008). Even though this method was apparently effective in some cases (e.g., Robertson and Grieve 1977, Grieve et al. 1991, Trepmann and Spray 2005), it did not really work properly with samples that underwent significant amounts of recrystallization (e.g., Grieve et al. 1990), or in samples that experienced relatively low shock pressure (e.g., Ferrière et al. 2008). Also it was shown that lithological properties of the investigated rock significantly influence the average pressure estimate (e.g., Grieve and Therriault 1995). On the other hand, another significant problem is directly related to the fact that, in most cases, planar microstructures are developed in areas that locally experienced pressures higher than the surroundings grains (which did not develop PDFs), and, thus, using such data may overestimate the "average" shock pressure of the sample.

In some cases the estimation of the relative shock-pressure differences was based on the abundance of shocked quartz grains and/or the average number of PDF sets per grain (e.g., Ferrière et al. 2008). However, because the percentage of shocked quartz grains in a sample also depends on the average grain size (with the larger grains tending to show more PDFs; e.g., Walzebuck and Engelhardt 1979, this study), such an estimate should be done with extreme care and following a very strict procedure. Being aware of all that, it is clear that the comparison of recorded shock levels between lithologically different samples is a very challenging task, unless the obtained values are normalized to the average area of the grains. But even if the percentage of the shocked quartz grains is normalized, it would not be sufficient because different PDF-bearing grains can be shocked to different extent. For example, two grains of similar size – the first with a very limited number of PDFs belonging to a single orientation in a limited portion of the grain, and the second grain fully covered with dense net of PDFs belonging to multiple orientations – were obviously not shocked to the same level.

Somewhat similar limitations also exist for the estimation of recorded shock pressure in a sample based on the average number of PDF sets per grain. Considering that in a given grain, two PDF sets can be either located in different parts of the grain or crosscutting sets, they may not necessarily be classified in the same way. For example, in some cases the development of these two different PDF orientations is clearly the result of Dauphiné twinning that already existed in the quartz grain before it was shocked. Consequently, it might be better to measure the average number of crosscutting PDF sets per grain instead of measuring the average number of PDF sets per grain. However, PDFs in the most highly shocked grains (Fig. 9) are often not clearly visible under an optical microscope because of the high density of planar

features and the highly distorted crystal lattice, leading to an underestimate of the average shock level.

We have demonstrated in our study that there is a need for an alternative method of estimation of the shock barometry in the case of highly heterogeneous, multigrain, multiminerale, and porous samples. This method should 1) appropriately consider the full spatial variability of the recorded shock pressures, 2) be relatively independent of the lithological differences, and 3) preferably not be more time-consuming than the currently used methods.

5. Conclusions

The following conclusions can be drawn from our study:

- 1) The distribution of PDF-bearing quartz grains is heterogeneous at the scale of a thin section on many different levels:
 - a) Within a single grain (with a uniform orientation of the crystal lattice) some portions of this grain are practically devoid of any sign of shock metamorphism, while other small (up to 20-30 μm in diameter) areas are highly shocked. The higher recorded shock level is due to a very high density of PDFs (expressed as number of planar features per unit area) that cross-cut each other (looking like “nests”). These are usually located either along cracks, or on the boundaries of the grains in contact with other type of minerals/material.
 - b) The heterogeneous distribution of grains bearing a similar number of PDFs is probably in large part derived from the random distribution of these “nests” within the quartz grains as described above.
- 2) Some zones of homogeneities within areas of the studied sample are also visible:
 - a) Some of the neighboring grains have a statistically significant similar number of PDF sets. This suggests (particularly the planar features present in most of these grains, not in the “nests”) that they were subjected to a similar stress field intensity.
 - b) Grains with PDF orientations along planes $\{10\bar{1}1\}$ and/or $\{11\bar{2}2\}$ tend to occur in groups. This clustering is a result of those grains being subjected to the local shock pressure appropriate for the development of these PDF orientations (probably above 5-10 GPa and below 25 GPa).
- 3) The orientation of the crystal lattice of the grains does not seem to be an important factor driving the development of PDFs in a specific location (at least not in samples from natural impact craters).
- 4) The PDFs developed along the $\{10\bar{1}1\}$ and $\{11\bar{2}2\}$ orientations are commonly poorly developed, hardly visible under the U-stage, and present on the grain margins as a few microns long planar and parallel features. This important difference of physical characteristics, appearance, and location within grain of different PDFs orientations, overlooked in previous studies, suggests that these PDFs may formed in a slightly

different mode than PDFs of more common orientations (such as the PDFs with $\{10\bar{1}3\}$ orientation).

- 5) The estimation of the recorded shock pressure from a given sample should be based on a) the average number of PDF sets present per grain, and/or b) the indexed PDF orientations, because these variables do not depend on the thoroughness of the analysis.

The program that was developed for this study allowing to fully automatically index PDFs in quartz grains is available online at: www.MeteorImpactOnEarth.com/ustage/program.html. The source code (i.e., implementation in Java programming language) is also available upon request from the authors.

Acknowledgments:

We acknowledge funding from the University of Vienna doctoral school IK-1045 and the Austrian Science Foundation grant P21821-N19. Authors are also very grateful for multiple interesting conversations about shock metamorphism with: Boris Ivanow, Uwe Reimold, Michael Poelchau, and Bevan French.

References

- Anselin L. 1999. Interactive techniques and exploratory spatial data analysis. In: Geographical Information Systems, edited by Longley P.A., Goodchild M.F., Maguire D.J, and Rhind D.W. New York: John Wiley & Sons. pp. 253–266.
- Baratoux D., and Melosh H. J. 2003. The formation of shatter cones by shock wave interference during impacting. *Earth and Planetary Science Letters* 2016: 43–54.
- Bowden E., Kondo K., Ogura T., Jones A. P., Price G. D., and DeCarli P. S. 2000. Loading path effects on the shock metamorphism of porous quartz (abstract #1582). *31st Lunar and Planetary Science Conference*. CD-ROM.
- Devore J., and Peck R. 1997. Statistics. The Exploration and Analysis of Data. Duxbury Press: Belmont. 256 p.
- Dressler B. O., Crabtree D., and Schuraytz B. C. 1997. Incipient melt formation and devitrification at the Wanapitei impact structure, Ontario, Canada. *Meteoritics & Planetary Science* 32: 249–258
- Dressler B. O., Sharpton V. L., and Schuraytz B. C. 1998. Shock metamorphism and shock barometry at a complex impact structure: State Islands, Canada. *Contributions to Mineralogy and Petrology* 130: 275–287.
- Engelhardt W. v., and Bertsch W. 1969. Shock induced planar deformation structures in quartz from the Ries crater, Germany. *Contributions to Mineralogy and Petrology* 20: 203–234.
- Ferrière L., Koeberl C., and Reimold W. U. 2007. Drill core LB-08A, Bosumtwi impact structure, Ghana: Petrographic and shock metamorphic studies of material from the central uplift. *Meteoritics and Planetary Science* 42: 611–633.

- Ferrière L., Koeberl C., Ivanov B., and Reimold W. U. 2008. Shock metamorphism of Bosumtwi impact crater rocks, shock attenuation, and uplift formation. *Science* 322: 1678–1681.
- Ferrière L., Morrow J. R., Amgaa T., and Koeberl C. 2009. Systematic study of universal-stage measurements of planar deformation features in shocked quartz: Implications for statistical significance and representation of results. *Meteoritics and Planetary Science* 44: 925–940.
- Ferrière L., Raiskila S., Osinski G. R., Pesonen L. J., and Lehtinen M. 2010. The Keuruselkä impact structure, Finland – Impact origin confirmed by characterization of planar deformation features in quartz grains. *Meteoritics and Planetary Science* 45: 434–446.
- Ferrière L., Lubala F. R. T., Osinski G. R., and Kaseti P. K. 2011. The newly-confirmed Luizi impact structure, Democratic Republic of Congo – Insights into central uplift formation and post-impact erosion. *Geology* 39: 851–854.
- French B.M. and Koeberl C. 2010. The convincing identification of terrestrial meteorite impact structures: What works, what doesn't, and why. *Earth-Science Reviews* 98: 123–170.
- Getis A. 1999. Spatial statistics. In: Geographical Information Systems, edited by Longley P. A., Goodchild M. F., Maguire D. J., and Rhind D. W. New York: John Wiley & Sons: pp. 239–251.
- Goltrant O., Doukhan J.-C., Cordier P., and Courtillot V. 1992. An investigation by transmission electron microscopy of planar deformation features in naturally shocked quartz. *Terra Nova* 4: 405–412.
- Goltrant O., Cordier P., and Doukhan J.-C. 1991. Planar deformation features in shocked quartz; a transmission electron microscopy investigation. *Earth and Planetary Science Letters* 106: 103–115.
- Grady D. E. 1980. Shock deformation of brittle solids. *Journal of Geophysical Research* 85: 332–338.
- Gratz A. J., Nellis W. J., Christie J. M., Brocious W., Swegle J., and Cordier P. 1992. Shock metamorphism of quartz with initial temperatures –170 to +1000°C. *Physics and Chemistry of Minerals* 19: 267–288.
- Grieve R. A. F., Langenhorst F., and Stöffler D. 1996. Shock metamorphism of quartz in nature and experiment: II. Significance in geoscience. *Meteoritics and Planetary Science* 31: 6–35.
- Grieve R. A. F. and Therriault A. M. 1995. Planar deformation features in quartz: Target effects. Proceedings, 26th Lunar and Planetary Science Conference: 515–516.
- Grieve R. A. F., Stöffler D., and Deutsch A. 1991. The Sudbury Structure: Controversial or misunderstood? *Journal of Geophysical Research* 96: 22753–22764.
- Grieve R. A. F., Coderre J. M., Robertson P. B., and Alexopoulos J. 1990. Microscopic planar deformation features in quartz of the Vredefort structure: Anomalous but still suggestive of an impact origin. *Tectonophysics* 171: 185–200.

- Grieve R. A. F. and Robertson P. B. 1976. Variations in shock deformation at the Slate Islands impact structure, Lake Superior, Canada. *Contributions to Mineralogy and Petrology* 58: 37–49.
- Güldemeister N., Wünnemann K., Duur N., and Hiermaier S. 2013. Propagation of impact-induced shock waves in porous sandstone using mesoscale modeling. *Meteoritics and Planetary Science* 48: 115–133.
- Holm S., Alwmark C., Alvarez W., and Schmitz B. 2011. Shock barometry of the Siljan impact structure, Sweden. *Meteoritics and Planetary Science* 46: 1888–1909.
- Hörz F. 1968. Statistical measurements of deformation structures and refractive indices in experimentally shock loaded quartz. In: *Shock metamorphism of natural materials*, edited by French B. M. and Short N. M. Baltimore: Mono Book Corporation. pp. 243–253.
- Huffman A. R. and Reimold W. U. 1996. Experimental constraints on shock-induced microstructures in naturally deformed silicates. *Tectonophysics* 256: 165–217.
- Huber M. S., Ferrière L., Losiak A., and Koeberl C. 2011. ANIE: A mathematical algorithm for automated indexing of planar deformation features in quartz grains. *Meteoritics and Planetary Science* 46: 1418–1424.
- Kennedy H. 2000. *Dictionary of GIS Terminology*. Redlands: Esri Press. 200 p.
- Kieffer S.W. 1971. Shock metamorphism of the Coconino Sandstone at Meteor Crater, Arizona. *Journal of Geophysical Research* 76: 5449–5473.
- Kieffer S. W., Phakey P. P., and Christie J. M. 1976. Shock processes in porous quartzite: transmission electron microscope observations and theory. *Contributions to Mineralogy and Petrology* 59: 41–93.
- Koeberl C., Milkereit B., Overpeck J.T., Scholz C. A., Amoako P. Y. O., Boamah D., Danuor S. K., Karp T., Kueck J., Hecky R. E., King J., and Peck J. A. 2007. An international and multidisciplinary drilling project into a young complex impact structure: The 2004 ICDP Bosumtwi impact crater, Ghana, drilling project—An overview. *Meteoritics and Planetary Science* 42: 483–511.
- Langenhorst F. 1994. Shock experiments on pre-heated α and β -quartz: II. X-ray and TEM investigations. *Earth and Planetary Science Letters* 128: 683–698
- Langenhorst F., and Deutsch A. 1994. Shock experiments on pre-heated α - and β -quartz: I. Optical and density data. *Earth and Planetary Science Letters* 125: 407–420.
- Langenhorst F. 2002. Shock metamorphism of some minerals: Basic introduction and microstructural observations. *Bulletin of the Czech Geological Survey* 77: 265–282.
- Robertson P. B., and Grieve R. A. F. 1977. Shock attenuation at terrestrial impact structures. In: *Impact and explosion cratering*, edited by Roddy D. J., Pepin P. O., and Merrill R. B. New York: Pergamon Press. pp. 687–702.
- Rogerson P. A. 2001. *Statistical Methods for Geography*. London: SAGE Publications. 248 p.

- Stöffler D., and Langenhorst F. 1994. Shock metamorphism of quartz in nature and experiment: I Basic observation and theory. *Meteoritics* 29: 155–181.
- Trepmann A., and Spray J. 2006. Shock-induced crystal-plastic deformation and post-shock annealing of quartz: microstructural evidence from crystalline target rocks of the Charlevoix impact structure, Canada. *European Journal of Mineralogy* 18: 161–173.
- Trepmann C. A. 2008 Shock effects in quartz: Compression versus shear deformation - An example from the Rochechouart impact structure, France. *Earth and Planetary Science Letters* 267: 322–332.
- Walzebuck J. P., and Engelhardt W. 1979. Shock deformation of quartz influenced by grain size and shock direction: Observations on quartz-plagioclase rocks from the basement of the Ries crater, Germany. *Contributions to Mineralogy and Petrology* 271: 267–271.

web sites of applied software:

<http://www-01.ibm.com/software/analytics/spss/> [date of collection 02.03.2011]

<http://www.esri.com/> [date of collection 02.03.2011]

ArcGIS Help Library 2010, ESRI

<http://onlinelibrary.wiley.com/doi/10.1111/j.1945-5100.2011.01234.x/supinfo>
[date of collection 02.05.2012]

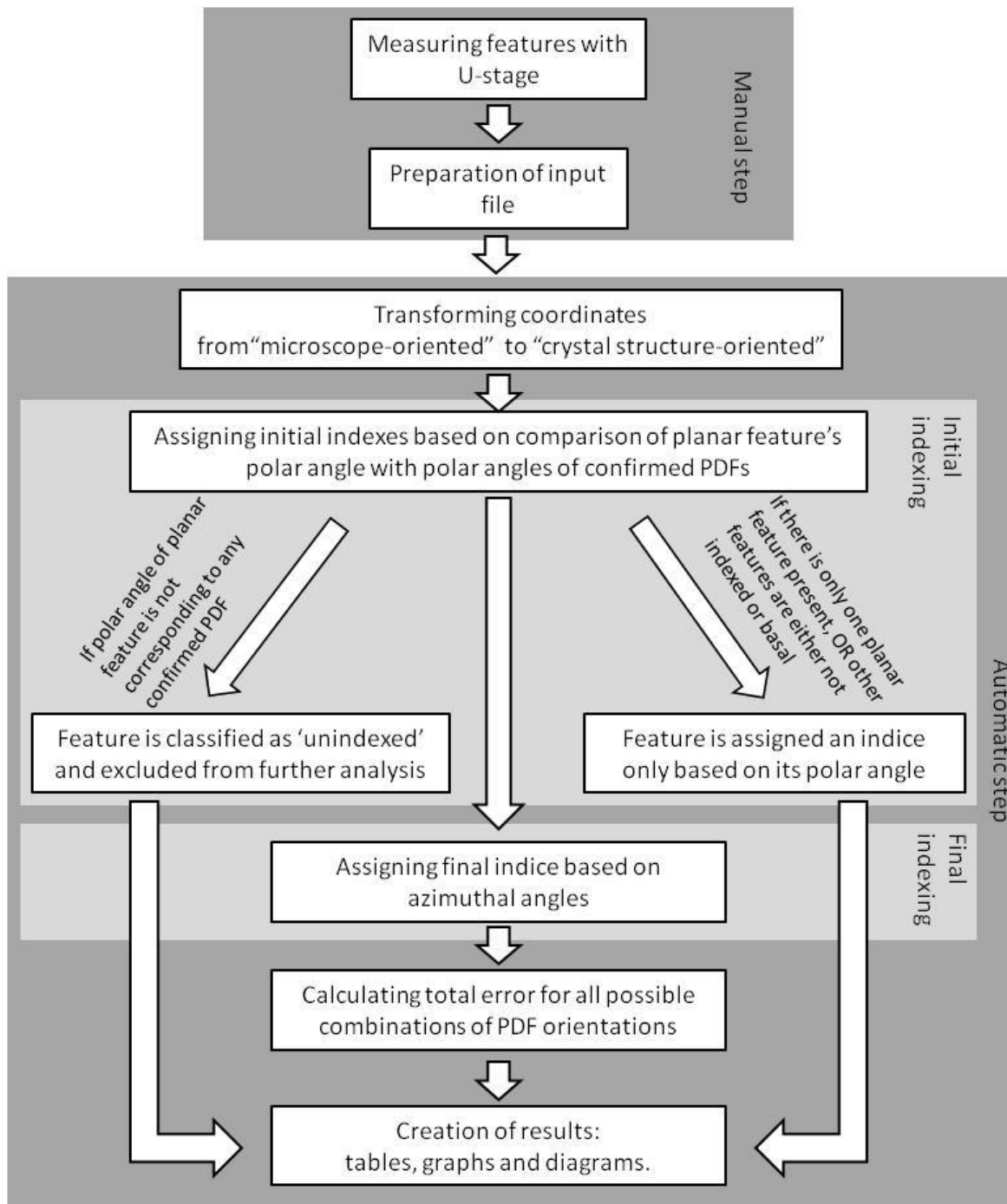


Fig. 2. Flowchart showing the algorithm of the web-based PDF indexing program presented in this paper.

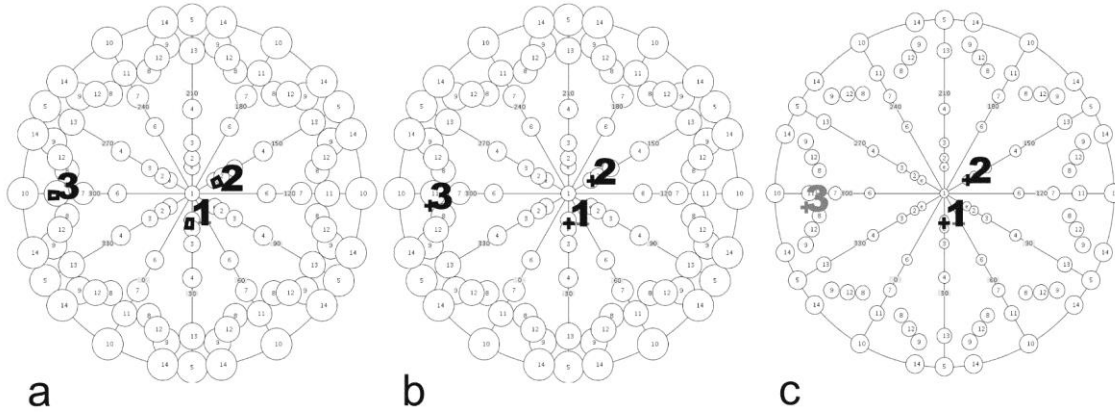


Fig. 3. Stereographic projection templates (after Ferrière et al. 2009) with the c-axis in the center and the circles representing the positions of the most common poles to PDF planes. These plots show a comparison of the resulting diagrams for a quartz grain with three planar features (marked as 1, 2, and 3, respectively) as produced using different program parameters: a) using the “min-max” method and a 5° error, b) using the “average” method and a 5° error, and c) using the “average” method and a 3° error. Note that in c) feature “3” is unindexed.

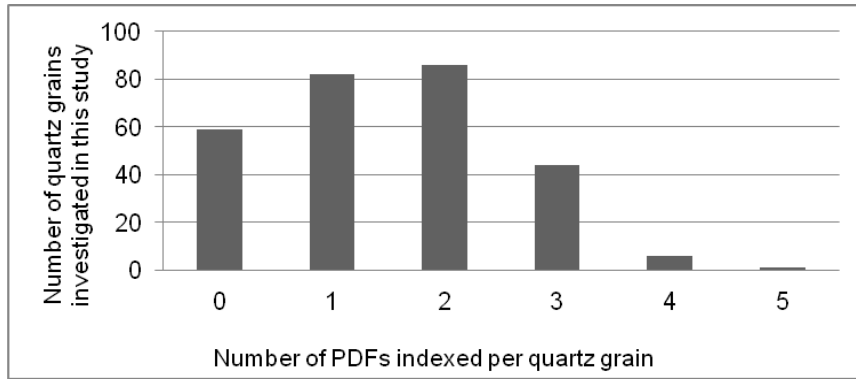


Fig. 4. Histogram showing the number of indexed PDF sets per quartz grain in the studied thin section of a shocked greywacke (KR8-029; Bosumtwi crater). This plot shows that most of the grains display only one or two indexed PDF sets. Only very few quartz grains include four or five PDF sets. The number of grains that do not display (indexed) PDFs is also represented on this histogram with the value "0".

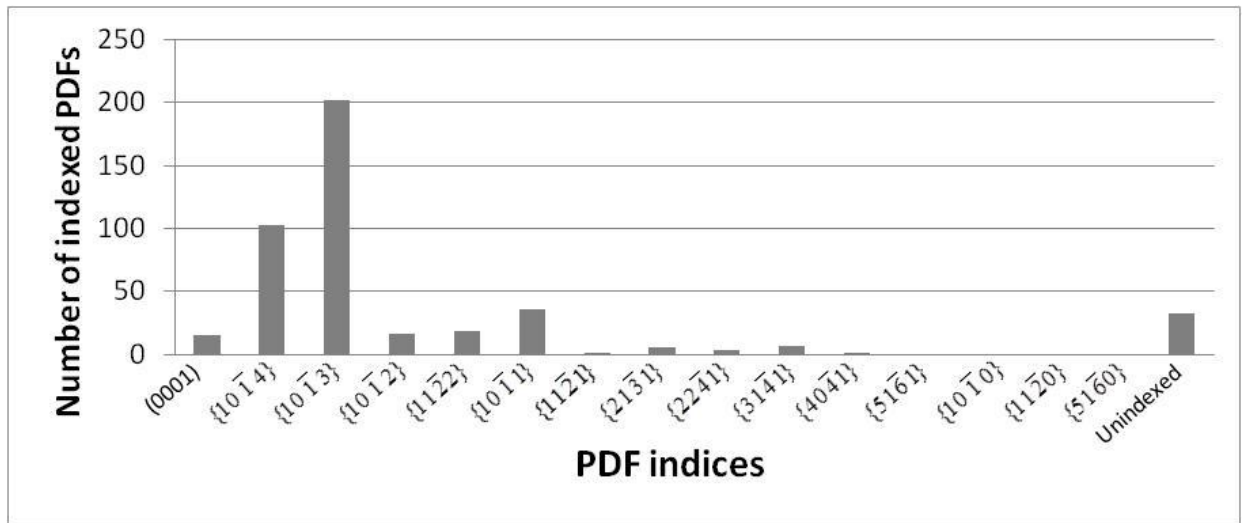


Fig. 5. Number and type of indexed PDF orientations in quartz grains (“min-max” method, 5° error) measured in the studied sample (KR8-029; Bosumtwi crater). The most common PDF orientations are {10 $\bar{1}$ 3} and {10 $\bar{1}$ 4} (45.8% and 23.4%, respectively), relatively common are also {10 $\bar{1}$ 1} and {11 $\bar{2}$ 2} orientations (8.2% and 4.1%, respectively). Only 7.5% of the measured features are unindexed.

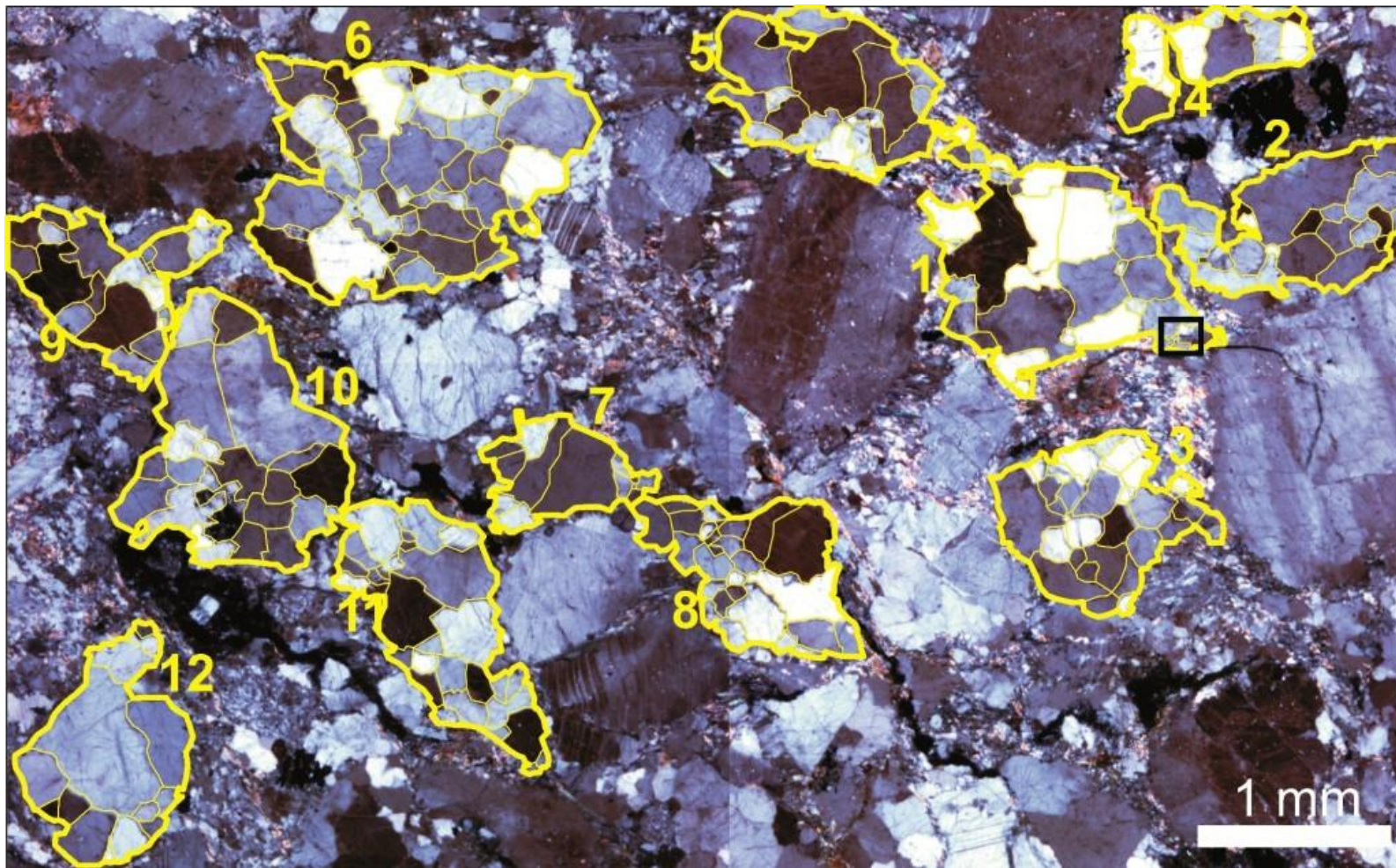


Fig. 6. Mosaic of microphotographs (in cross-polars) of the investigated thin section of the sample KR8-29 (from the LB-08A drill core; Bosumtwi crater). The exact same area as on the following figures is depicted here with the outline and identification numbers of the different clusters that we have defined. The black rectangle (upper right) shows the location of the Fig. 9.

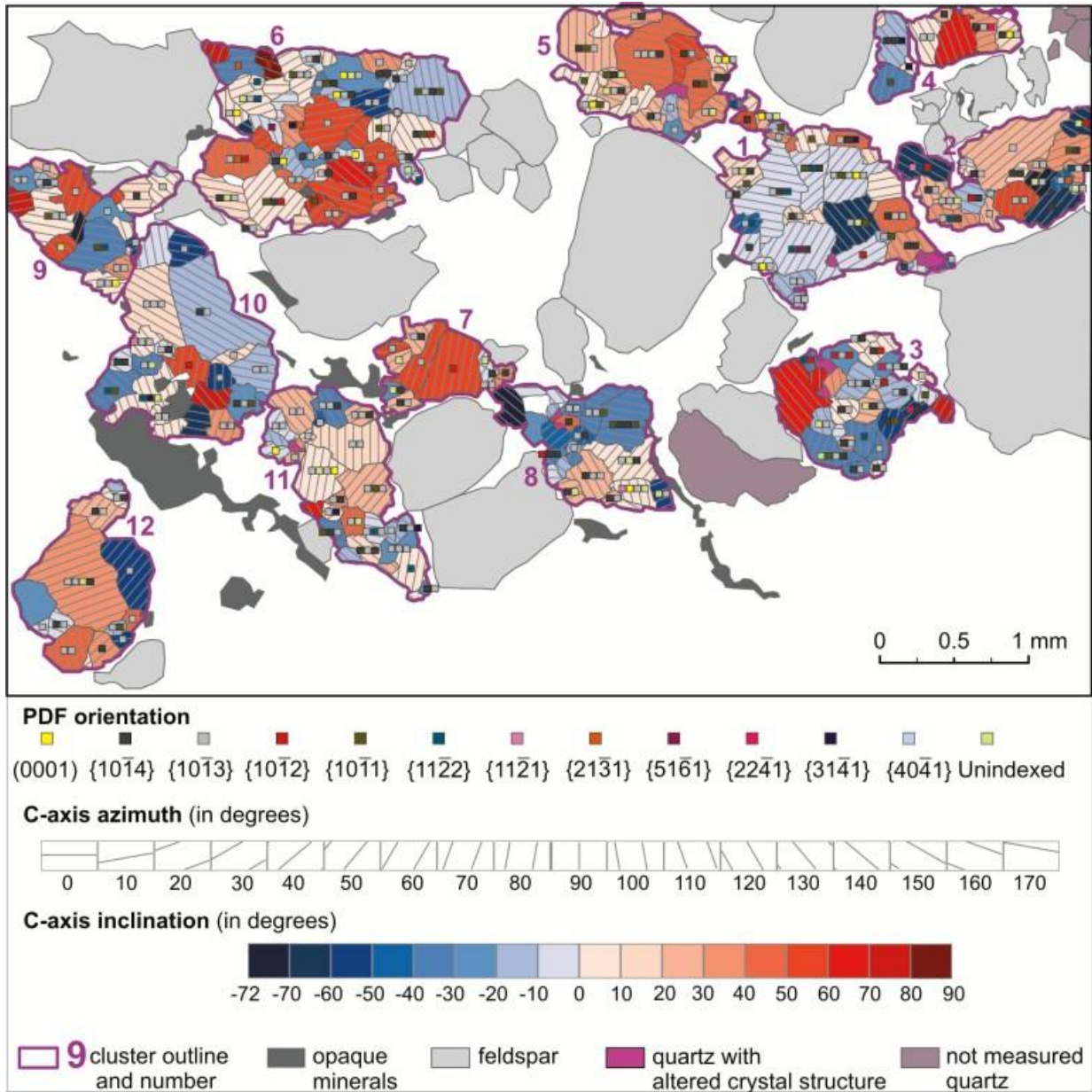


Fig. 7. Detailed map of the clusters of quartz grains as mapped in sample KR8-29; from the Bosumtwi crater). The orientation of the crystal lattice of the measured quartz grains as well as the number and orientations of the indexed PDFs is shown. In some cases the c-axis of the quartz grains could not be measured because it is too damaged (it is marked as “quartz with altered crystal structure”).

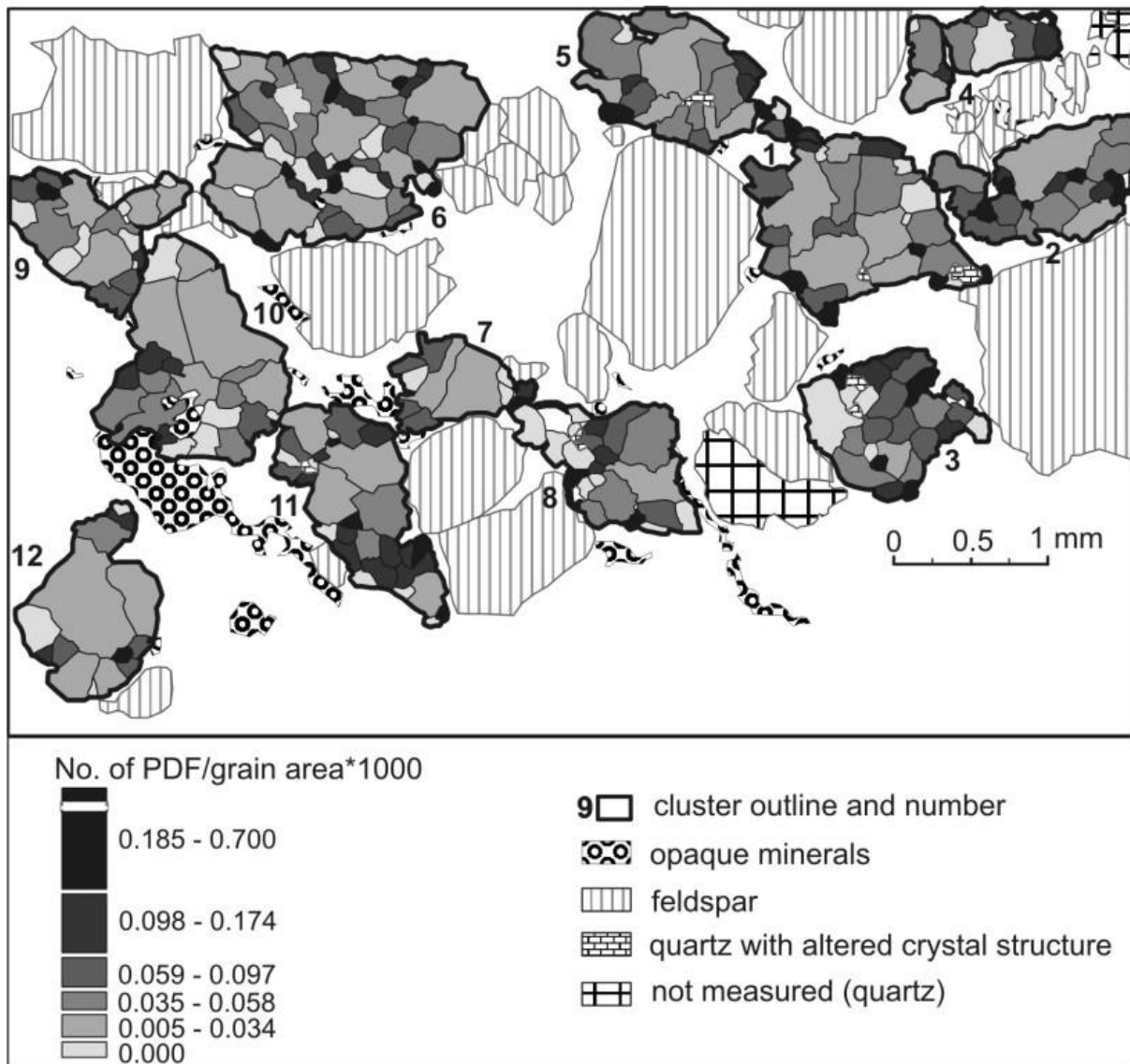


Fig. 8. Abundance of PDFs per quartz grains (i.e., number of PDFs per grain area) in sample KR8-29 (Bosumtwi crater). The average density of PDF sets per grain-area shows an over-representation of small quartz grains with a very high density of PDF sets per grain-area. This can be explained by either the rotation of part of the crystals previously being part of larger grains, due to extensive shock or a computational artifact (i.e., a single PDF set in one grain gives higher set density than 4 sets within a very large grain). In some cases the c-axis of the quartz grains could not be measured because it is too damaged (it is marked as “quartz with altered crystal structure”).

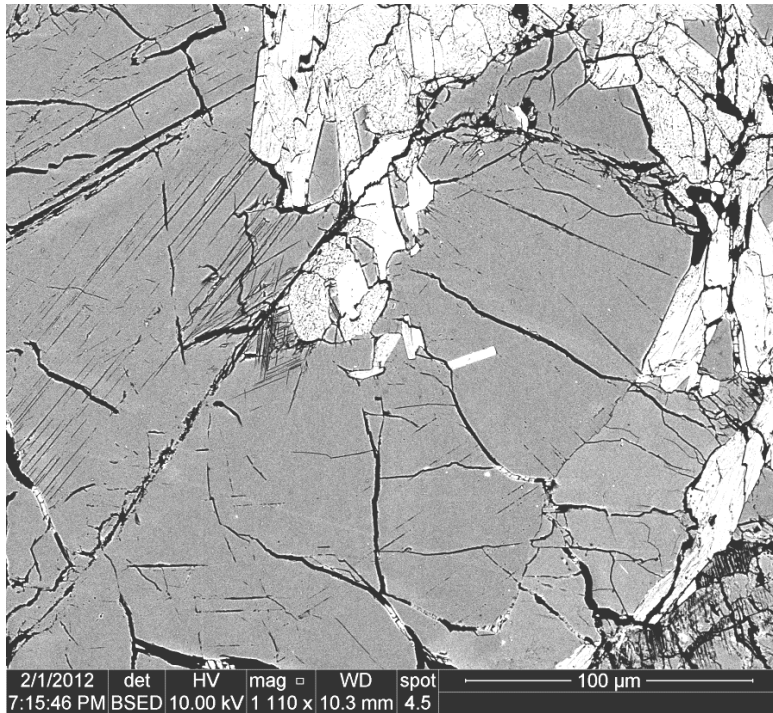


Fig. 9. Backscattered electron image showing a particular sector of cluster #1 indicated in Fig. 6. The grey grains in the center and to the left are quartz with planar deformation features. Most of the quartz includes widely spaced PDFs or no planar features at all. The area in the center left includes tightly spaced PDFs (two or more sets in the exact same place). This probably illustrates a local maximum within the heterogeneous stress field produced by shock wave propagation through a heterogeneous sample.

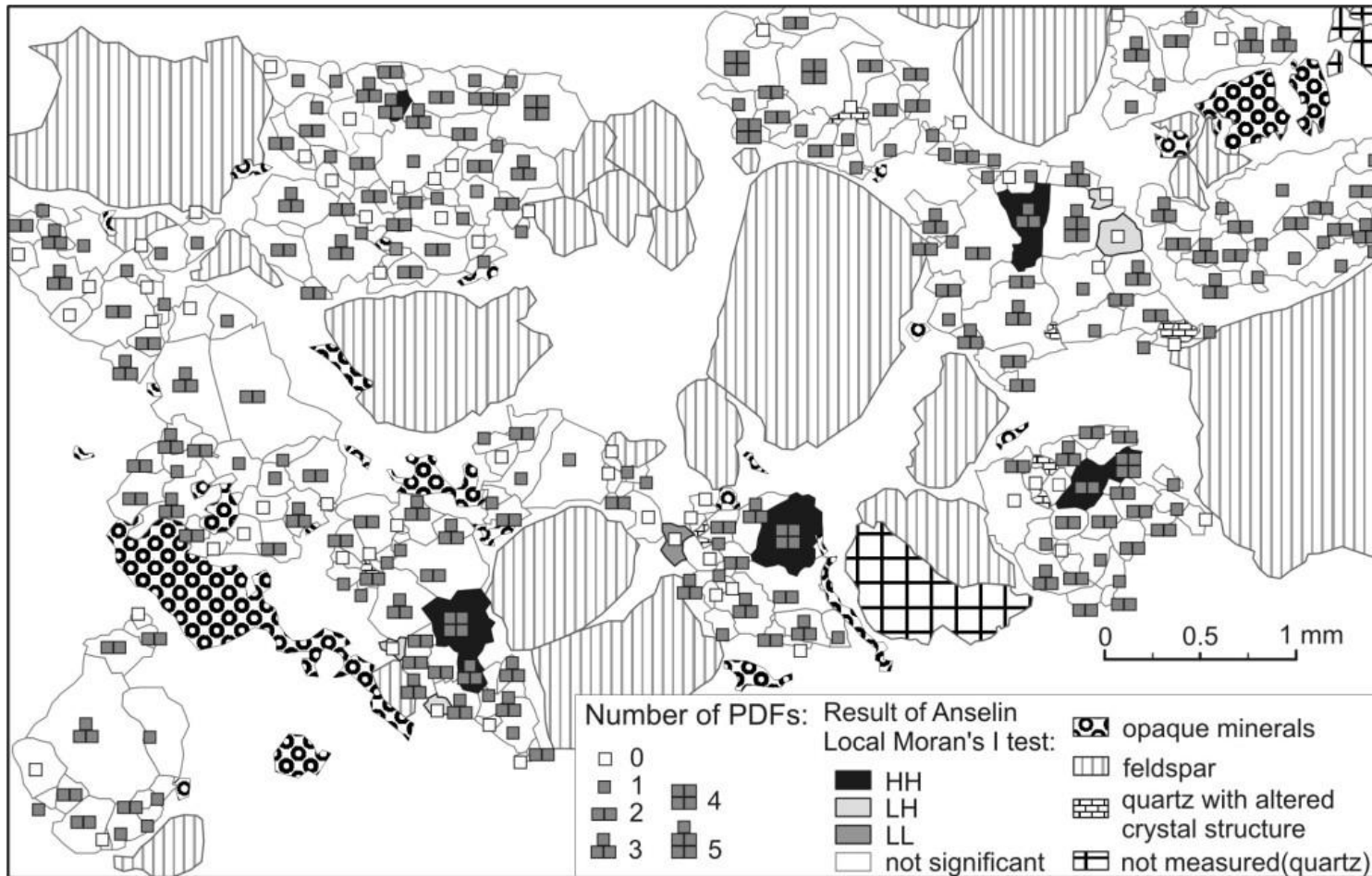


Fig. 10. Map showing result of Anselin Local Moran's test on quartz grains from sample KR8-29 (Bosumtwi crater). This test allows to identify clusters of grains with high number of PDFs (marked as HH), clustering of grains with small number of PDFs (marked as LL), and spatial outliers; e.g., grains with a high number of PDFs surrounded by grains with a small number of PDFs (marked as HL). The results of this analysis show that several grains yield statistically significant results, thus, indicating that in some cases grains with high, or low, number of PDFs present are spatially clustered. This probably illustrates a local maximum within the heterogeneous stress field produced by shock wave propagation through a heterogeneous sample. In some cases the c-axis of the quartz grains could not be measured because it is too damaged (marked as "quartz with altered crystal structure").

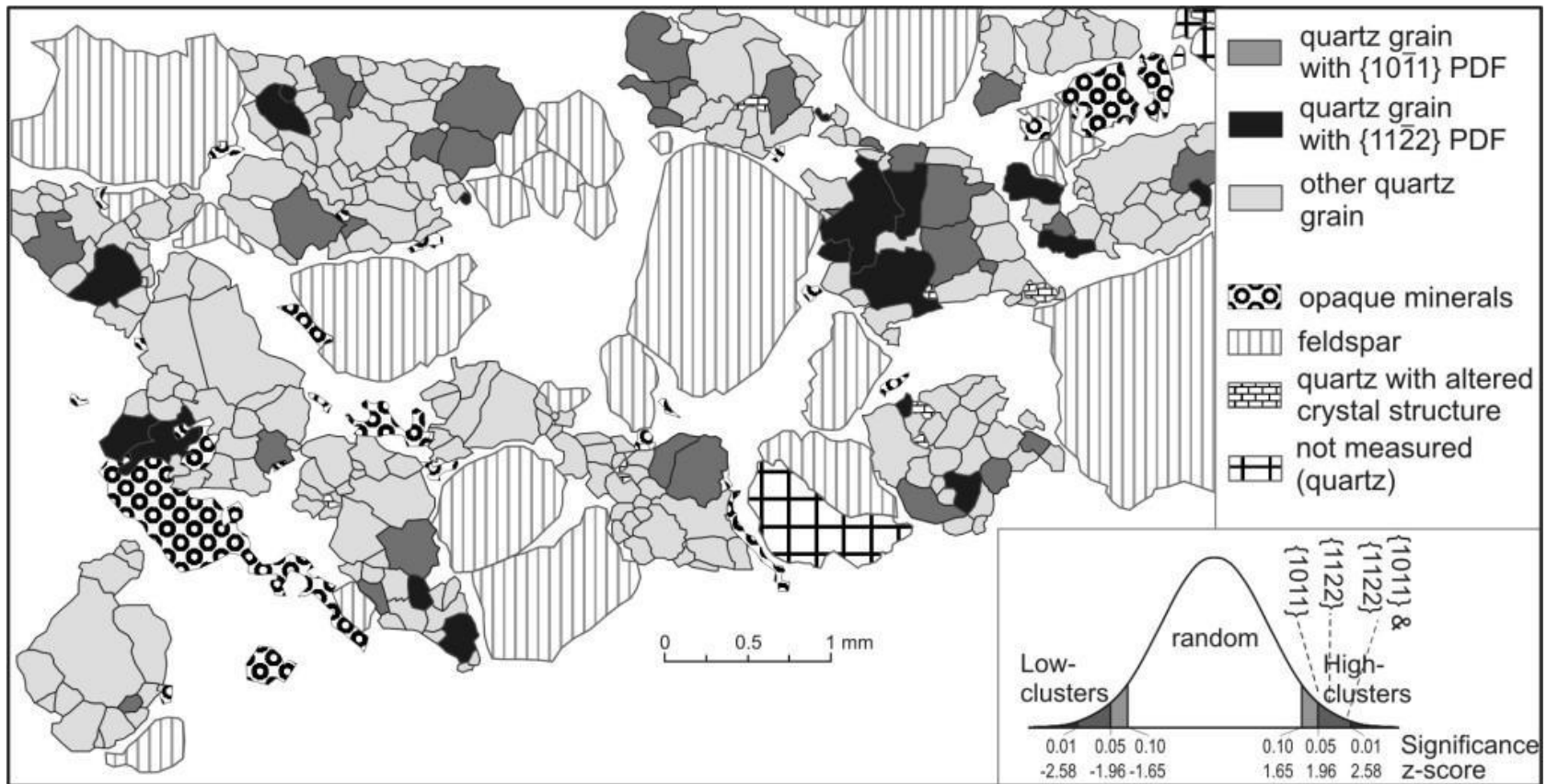


Fig. 11. Map of location of grains with PDF orientations $\{10\bar{1}1\}$ and $\{11\bar{2}2\}$ in sample KR8-29 (Bosumtwi crater). The results of the Getis-Ord General G statistical analysis is also provided here, showing that quartz grains with these two particular orientations of PDFs tend to occur in clusters that are not random on the 2σ significance level. In some cases the c-axis of the quartz grains could not be measured because it is too damaged (marked as “quartz with altered crystal structure”).

Tables

Tab. 1. Comparison of results for a sample from the Bosumtwi crater (sample BOS-3; data previously published in Ferrière et al. 2009) indexed with our web-based program, using the two available error handling methods; i.e., the "min-max" method (the algorithm uses values from the entire interval) and the "average" method (the algorithm calculates the average value of the entire measured interval, and the indexing is performed using this "average value") and three different error rates (distance from a classified PDF orientation that will still be counted as properly indexed), 3°, 5°, and 7°. Data is given here as number of PDFs.

Method	Error rate	(0001)	$\{10\bar{1}4\}$	$\{10\bar{1}3\}$	$\{10\bar{1}2\}$	$\{11\bar{2}2\}$	$\{10\bar{1}1\}$	$\{11\bar{2}1\}$	$\{21\bar{3}1\}$	$\{22\bar{4}1\}$	$\{31\bar{4}1\}$	$\{40\bar{4}1\}$	$\{51\bar{6}1\}$	$\{10\bar{1}0\}$	$\{11\bar{2}0\}$	$\{51\bar{6}0\}$	Un-indexed
min-max	3°	0	28	51	28	2	6	2	2	6	3	1	3	1	1	0	11
min-max	5°	0	29	53	29	2	8	2	2	7	3	1	2	1	1	0	5
min-max	7°	0	30	54	30	1	9	2	3	7	4	0	1	1	1	0	2
average	3°	0	27	37	20	2	4	0	1	2	4	3	1	1	0	0	43
average	5°	0	30	45	24	2	7	1	4	5	3	2	2	1	0	0	19
average	7°	0	30	50	28	2	7	2	5	6	2	1	1	1	1	0	9

Tab. 2. Comparison between manually (by L. Ferrière) and automatically indexed PDFs (using our web-based program) from five samples from five different impact structures (from: ¹Ferrière et al. 2009, ²Ferrière et al. 2011, ³Ferrière et al. 2010). Data is given here as number of PDFs.

Crater, lithology	Method	(0001)	{10 $\bar{1}$ 4}	{10 $\bar{1}$ 3}	{10 $\bar{1}$ 2}	{11 $\bar{2}$ 2}	{10 $\bar{1}$ 1}	{11 $\bar{2}$ 1}	{21 $\bar{3}$ 1}	{22 $\bar{4}$ 1}	{31 $\bar{4}$ 1}	{40 $\bar{4}$ 1}	{51 $\bar{6}$ 1}	{10 $\bar{1}$ 0}	{11 $\bar{2}$ 0}	{51 $\bar{6}$ 0}	Un-indexed	Total
Gosses Bluff ¹ , sandstone	program	59	39	70	2	2	13	1	2	2	2	1	2	1	0	1	11	208
	manual	59	110		2	5	10	0	3	0	3	2	1	1	1	1	1	10
Bosumtwi ¹ , meta-greywacke	program	0	29	53	29	2	8	2	2	7	3	1	2	1	1	0	5	145
	manual	0	81		28	4	5	2	3	6	3	2	1	1	1	0	8	145
Manson ¹ , biotite-gneiss	program	4	46	117	4	2	15	0	5	10	2	1	0	0	0	1	5	212
	manual	4	166		2	3	13	0	3	10	2	2	1	0	0	1	5	212
Luizi ² , sandstone	program	12	45	116	8	0	0	0	0	1	0	0	0	0	0	0	3	185
	manual	12	163		5	0	0	0	0	0	0	0	0	0	0	0	5	185
Keurusselk ä ³ , ortho-gneiss	program	0	61	66	1	0	0	0	0	0	0	0	0	0	0	0	1	129
	manual	0	124		1	0	0	0	0	0	0	0	0	0	0	0	4	129

Tab. 3. Crystallographic orientations of PDFs in quartz grains in meta-greywacke sample KR8-029 from the Bosumtwi crater as measured in this study and compared to previous results by Ferrière et al. (2008).

PDF orientation		(0001)	$\{10\bar{1}4\}$	$\{10\bar{1}3\}$	$\{10\bar{1}2\}$	$\{11\bar{2}2\}$	$\{10\bar{1}1\}$	$\{11\bar{2}1\}$	$\{21\bar{3}1\}$	$\{22\bar{4}1\}$	$\{31\bar{4}1\}$	$\{40\bar{4}1\}$	$\{51\bar{6}0\}$	Un indexed	Total
This study	Number of PDFs	15	103	202	16	18	36	1	6	3	7	1	0	33	441
	% of PDF orientations	3.4	23.4	45.8	3.6	4.1	8.2	0.2	1.4	0.7	1.6	0.2	0.0	7.5	100.0
Ferrière et al. (2008)	Number of PDFs	1	-	56	2	1	0	0	0	-	-	-	-	1	61
	% of PDF orientations	1.6	-	91.8	3.3	1.6	0.0	0.0	0.0	-	-	-	-	1.6	100.0

Tab. 4. Basic data on the performed measurements of PDF sets present within quartz grains in sample KR8-29 (Bosumtwi crater). Data are shown for each cluster as number of PDFs, unless indicated otherwise.

	Total	Cluster number no.											
		1	2	3	4	5	6	7	8	9	10	11	12
Entire sample													
Area of cluster [μm ²]	34054169	1122954	675038	671447	326923	715248	1632088	329836	621749	555552	1106398	767885	695132
No. of grains	278	33	20	25	9	17	52	12	23	19	21	29	14
Mean area of a grain [μm ²]	32651	33299	33378	25231	35330	41268	30418	27448	25793	29145	50536	26286	49657
St. dev. of area of cluster	37999	40341	39699	20488	22302	38060	31113	36084	26207	25528	55796	28768	73438
No. of PDFs	409	54	36	42	14	32	75	12	27	21	31	47	18
Mean no. of PDFs	1.47	1.64	1.80	1.68	1.56	1.88	1.44	1.00	1.17	1.11	1.48	1.62	1.29
St. deviation of no. of PDFs	1.09	1.18	0.75	1.01	1.17	1.02	1.01	0.71	1.31	1.07	1.05	1.22	0.88
Mean no. of PDFs in a grain	1.47	1.64	1.80	1.68	1.56	1.88	1.44	1.00	1.17	1.11	1.48	1.62	1.29
No. of grains without PDFs	61	6	1	4	2	1	11	3	11	7	5	7	3
PDF indices													
(0001)	15	3	0	0	1	2	5	0	1	1	0	2	0
{10 $\bar{1}$ 4}	103	13	9	13	5	10	17	5	10	2	5	9	5
{10 $\bar{1}$ 3}	203	23	16	17	4	15	33	6	12	15	20	30	12
{10 $\bar{1}$ 2}	16	1	3	5	0	0	4	1	1	0	1	0	0
{10 $\bar{1}$ 1}	36	8	2	3	1	5	8	0	3	1	2	2	1
{11 $\bar{2}$ 2}	18	5	3	2	0	0	3	0	0	1	2	2	0
{11 $\bar{2}$ 1}	1	0	1	0	0	0	0	0	0	0	0	0	0

{21 $\bar{3}$ 1}	6	1	1	0	0	0	4	0	0	0	0	0	0
{22 $\bar{4}$ 1}	3	0	0	2	1	0	0	0	0	0	0	0	0
{31 $\bar{4}$ 1}	7	1	0	0	2	0	1	0	0	0	1	2	0
{40 $\bar{4}$ 1}	1	0	1	0	0	0	0	0	0	0	0	0	0
Unindexed	33	3	4	3	0	4	4	3	5	1	3	2	1
Pearson's product moment	0.39	0.60	-0.05	0.02	0.42	0.59	0.51	0.06	0.61	0.48	0.32	0.51	0.54